AIAA SciTech Forum
8–12 January 2018, Kissimmee, Florida
2018 AIAA Aerospace Sciences Meeting

10.2514/6.2018-0056

HIFiRE-1 and -5 Flight and Ground Tests

Roger L. Kimmel,[*] David Adamczak,[†] Matthew P. Borg,[‡]
Air Force Research Laboratory, 2130 8th St., WPAFB, OH 45433, USA

Joseph S. Jewell[§],
Air Force Research Laboratory and Spectral Energies, LLC, Dayton, OH, United States,

Thomas J. Juliano,[**]
University of Notre Dame, Notre Dame, IN, United States

Scott Stanfield,[††]
Innovative Scientific Solutions, Inc., Dayton, OH, United States

Karen Berger[‡‡]
NASA Langley Research Center, Hampton, VA, United States

The Hypersonic International Flight Research Experimentation (HIFiRE) program is a hypersonic flight test program executed by the Air Force Research Laboratory (AFRL) and Australian Defence Science and Technology Group (DSTG), including flight, ground test and computation. HIFiRE flights one and five were devoted to boundary-layer transition. The body of knowledge from the research campaigns shows a complex transition behavior. Axisymmetric flows and crossflow transition were strongly affected by wind tunnel noise, with transition occurring at lower Reynolds numbers in the wind tunnel. Similarly, three-dimensional flows with inflected velocity profiles, such as the leeward side of HIFiRE-1, or the HIFiRE-5 centerline, exhibited much lower transition Reynolds numbers in ground test, compared to flight. The disparity between flight and wind tunnel transition Reynolds numbers was less pronounced for attachment-line transition. The supposition is that this transition mechanism was either less affected by wind tunnel noise, or were more susceptible to disparities in wall cooling between wind tunnel and flight.

Nomenclature

f = frequency, units as noted
h = convective heating coefficient
$h_{F\text{-}R}$ = reference convective heating coefficient
M = Mach number, dimensionless
N = dimensionless disturbance amplitude, $\ln(A/A_0)$, where A_0 is amplitude at lower neutral bound
$\mathrm{Re_e}$ = unit Reynolds number based on boundary-layer edge conditions, per meter
$\mathrm{Re_{RN}}$ = Reynolds number based on freestream (upstream of bow shock) conditions and nose radius
$\mathrm{Re_x}$ = Reynolds number based on freestream (upstream of bow shock) conditions and axial length
$\mathrm{Re_{x,tr}}$ = transition Reynolds number based on freestream (upstream of bow shock) conditions and axial length
T_w = wall temperature, K
T_0 = stagnation temperature, K
t = time, seconds
x = axial length, units as noted

[*] Principal Aerospace Engineer, Associate Fellow AIAA.
[†] Senior Engineer, Senior Member AIAA
[‡] Aerospace Engineer, Senior Member, AIAA
[§] Aerospace Engineer, Senior Member, AIAA
[**] Assistant Professor, University of Notre Dame, Notre Dame, IN, United States, Senior Member, AIAA
[††] Aerospace Engineer, Member, AIAA
[‡‡] Aerospace Engineer, Associate Fellow, AIAA

Cleared for public release, 88ABW-2017-5704, 14 November 2017

y = spanwise distance, units as noted
x_T = transition location, meters
α = angle-of-attack, degrees
Φ = azimuthal coordinate in wind-fixed reference frame, degrees
ϕ = azimuthal coordinate in body-fixed coordinate system, degrees

I. Introduction

The Hypersonic International Flight Research Experimentation (HIFiRE) program is a hypersonic flight test program executed by the Air Force Research Laboratory (AFRL) and the Australian Defence Science and Technology Organization (DSTO).[1,2] Its purpose is to develop and validate technologies critical to next generation hypersonic aerospace systems. Candidate technology areas include, but are not limited to, propulsion, propulsion-airframe integration, aerodynamics and aerothermodynamics, high temperature materials and structures, thermal management strategies, guidance, navigation, and control, sensors, and system components. The HIFiRE program consists of extensive ground tests and computation focused on specific hypersonic flight technologies. Each technology program culminates in a flight test.

Two HIFiRE flights focused on boundary-layer transition. HIFiRE-1 created an extensive knowledge base regarding transition on axisymmetric bodies that was summarized in numerous prior publications.[3-17] HIFiRE-5 was devoted to measuring transition on a three-dimensional (3D) body. The results of this flight were summarized in a number of technical papers.[18- 23] Preflight research was described in numerous publications.[24-40]

Both HIFiRE transition flight experiments were successful, with some minor anomalies. HIFiRE-1 launched 22 March 2010 at the Woomera Prohibited Area in South Australia. This vehicle entered the atmosphere at higher-than-intended angle-of-attack, but was otherwise successful. Low angle-of-attack (AoA) hypersonic transition data were obtained on ascent, and high AoA transition was measured during descent. The HIFIRE-5a mission launched 23 April 2012 from Andoya, Norway.[41-44] The second stage of HIFiRE-5a failed to ignite, preventing the payload from attaining hypersonic speeds. Despite the failure of the HIFiRE-5a second stage, the payload acquired supersonic transition data. However, since this did not satisfy mission objectives to acquire hypersonic transition measurements, a new payload, essentially identical to the first, was constructed and flown at Woomera, Australia, on 18 May 2016. This mission, HIFiRE-5b, was entirely successful.

The HIFiRE-1 and -5 primary experimental objectives were to measure transition on smooth bodies in hypersonic flight. Although previous flight tests had measured transition during hypersonic flight tests, these tests were subject to some ambiguity due to surface roughness, as-flown nosetip geometry, vehicle motion, ablation, wall temperature and so on. Schneider provides a survey paper of previous hypersonic flight test.[45] The HIFiRE goal was to remove this ambiguity by flying heavily-instrumented test articles with smooth, unablating moldlines. The singular flight test product that could not be derived from ground test was transition measurements in a quiet environment. Transition locations measured in flight would be converted to transition Reynolds numbers and *N*-factors, and compared to ground test results to assess the influence of wind tunnel noise, and to provide some calibration of *N*-factor prediction methods. Subsequent sections of this paper will demonstrate that this goal was achieved, and will summarize conclusions regarding ground test and computation that could be derived from the flight data.

The HIFiRE research program obtained data on numerous aspects of hypersonic transition, including roughness-dominated transition and the phenomenology of transition in flight. To limit the scope of this paper, only smooth-body results are discussed, with a focus on comparison to ground test and computation. The research campaign also contributed a huge amount of computational work. For brevity, discussion of computational results is limited to a few select computations that help elucidate the flight and ground transition results.

II. Flight Experiments Description

The HIFiRE-1 and -5 configurations were described in a prior papers.[16, 41] Both configurations consisted of an instrumented test article mounted atop a two-stage, ground-launched sounding rocket. The payloads remained attached to the second stage throughout flight. The vehicles were spun at a low rate to reduce trajectory dispersion. Cant-angle on the first and second-stage fins caused the vehicles to spin passively. Because of this, the vehicles were rolling throughout the entire trajectory. Both flights were launched with high elevations and flew lofted, ballistic trajectories, with short endoatmospheric flight times, and with relatively long exoatmospheric stages and high exoatmospheric apogees. Data were obtained on ascent and descent, with descent being the primary test window.

Neither flight possessed active control surfaces on the upper stage, and relied solely on the static aerodynamic stability of the stack to maintain low angle-of-attack during ascent. During relevant ascent flight periods, angle-of-attack was less than 0.5°. On both flights, cold-gas thrusters were used during exoatmospheric flight to orient the

vehicle along the descent flight path vector, in order to minimize angle of attack during descent. This maneuver was unsuccessful for HIFiRE-1, and the payload reentered the atmosphere at a relatively high angle of attack. The AoA damped in an oscillatory manner so that $5° < \alpha < 13°$ during descent transition. The HIFiRE-5b exoatmospheric thruster maneuver was successful, so that AoA during descent transition was less than 1°. Considerable effort was expended to ensure that the HIFiRE-1 and -5 instrumentation and post-flight analysis were able to resolve the effects of the vehicle motion.

The 7-degree half-angle cone geometry was chosen for HIFiRE-1 since this configuration had been the basis of extensive test and analysis for many years. The HIFiRE-5 configuration was chosen as the test-article geometry based on extensive previous testing and analysis on elliptic cones.[46-53] This prior work[46-48] demonstrated that the 2:1 elliptic cone would generate significant crossflow instability at hypersonic flight conditions and potentially exhibit leading-edge transition. Figure 1, taken from Refs. 16 and 18 illustrates the HIFiRE-1 and -5 geometries.

Both payloads consisted of aluminum frusta that served as the primary test surfaces, and had solid, uninstrumented nosetips built-up from several materials. To account for the differential coefficients of thermal expansion of the nosetip materials, the tips possessed backward-facing steps at each material interface when cold. The steps were sized to approach zero height when the nosetip was at working temperature in the test window during descent. The nosetips of both vehicles were slightly blunted. Refs. 10, 16, and 18 describe the nosetip details and detailed surface roughness measurements. For both HIFiRE-1 and -5, roughness did not demonstrably affect transition, and nose-bluntness effects were limited primarily to the first 300 mm of the test article.

The bulk of the instrumentation on both flights consisted of Medtherm coaxial thermocouples, hand-contoured to the outer mold line of the vehicle. The HIFiRE-1 test surface contained two rays of thermocouples. The secondary side of the vehicle possessed a diamond-shaped discrete roughness element to assess tripped transition, and the primary side of the cone was smooth. The HIFiRE-5 configuration had one side that contained a closeout panel with fasteners. The primary test surface on the other side was smooth and devoid of fasteners. Ground tests verified on both vehicles that roughness-induced transition would not contaminate the test surface flow. Post flight analysis confirmed that this indeed was the case.

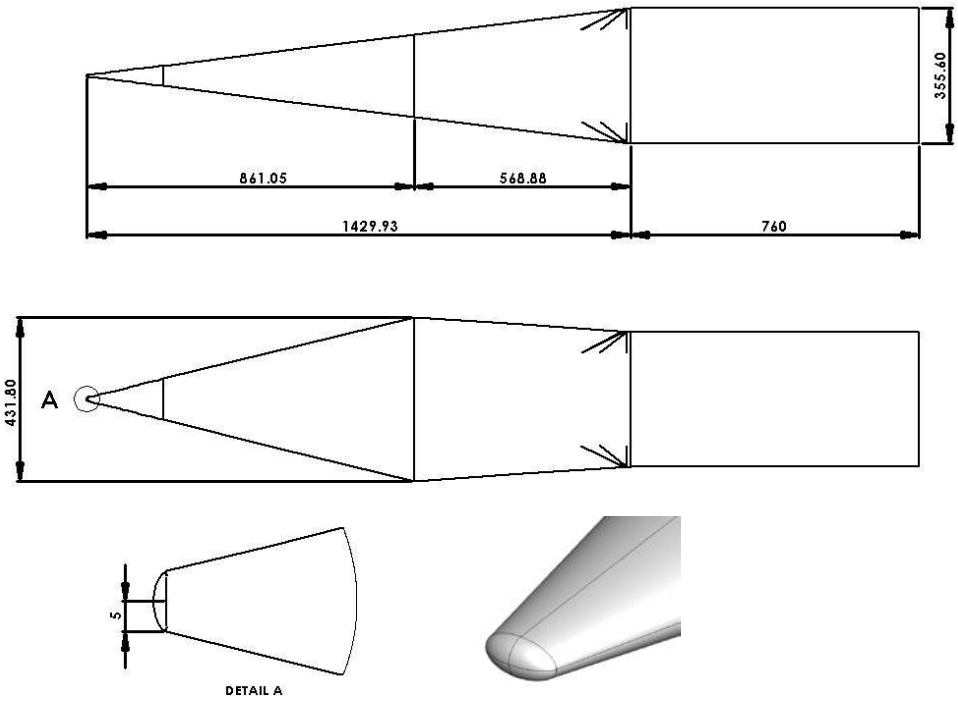

Figure 1 HIFiRE-1 (top, Ref. 16) and HIFiRE-5 (bottom, Ref. 18) flight vehicles.

III. Smooth-Body, Axisymmetric Transition – HIFiRE-1

During ascent, flow over the HIFiRE-1 test article was turbulent immediately after launch. As the vehicle ascended, and Reynolds number dropped, transition moved aft over the vehicle. Ascent transition occurred in three

phases. In phase one, for $t < 15$ s, roughness due to nosetip joint steps dominated transition. For $t > 15$ s, the combination of higher nose temperature, which reduced step heights, and lower Reynolds number and higher Mach number, which made the boundary-layer less sensitive to roughness, lessened the influence of the steps. However, during phase two, $15 < t < 19$ s, nosetip roughness still appeared to affect transition somewhat, and transition behaved erratically. During phase three, $19 < t < 22$ s, transition on the primary test surface moved downstream in an orderly fashion, consistent with a smooth-body transition, with $10.4\times10^6 < Re_x < 13.7\times10^6$. For $t > 22$ s during ascent, the primary test surface was entirely laminar. During phase three, AoA was estimated to be less than 0.5°, and the ratio of wall-temperature to stagnation-temperature was approximately 0.3. Flow downstream of the diamond-shaped trip on the secondary instrument ray remained turbulent until $t \sim 30$ s, after which it was laminar for the remainder of the ascent.

During phase three (smooth-body transition), transition occurred at conditions where Mack's second-mode was predicted to dominate.[54] Boundary-layer stability analysis at intervals during $19 < t < 22$ s indicated second-mode N-factors at transition of $10.9 < N < 14.5$, with an average value of N=13.4. The frequency corresponding to the peak N-factor at transition during this period was calculated to be $400 < f < 725$ kHz. The transition N-factor calculated for t=19s (N=10.9) was low and slightly out-of-family with transition N-factors at later times. For $20 < t < 22$s, $13 < N < 14.5$.

The HIFiRE-1 ascent transition N-factors were broadly consistent with past hypersonic flight tests, that is to say, at the upper end of commonly-cited free-flight transition N-factors. Ref. 16 includes a brief comparison of HIFiRE-1 to previous tests. Stability calculations by multiple researchers for the Reentry-F and Sherman-Nakamura hypersonic flight tests indicated correlating transition N-factors of 3.7-15.[55, 56] The investigators ascribed much of this variation to uncertainty in the calculated boundary conditions. With the lowest Reentry-F transition N-factor excluded, correlating transition N-factors for these two flights ranged from 8-15.

The HIFiRE-1 transition measurements may be used, judiciously, to inform hypersonic transition design. The final transition prediction depends on the designer's risk tolerance. Based on the above data, it is reasonable to conclude that for a smooth, axisymmetric body, where ablation is not dominant, $8 < N < 15$ would be reasonable correlating N-factors for second-mode transition in hypersonic flight. This is an aggressive stance and probably approaches an upper limit on attainable laminar Reynolds number for these bodies under optimistic conditions. Depending on the desired level of conservatism, lower transition Reynolds numbers might be appropriate to account for uncertainty in flight conditions, surface geometry, or the potential for other "bypass" transition mechanisms.

A practical design question is the uncertainty in the transition location to which this N-factor uncertainty equates. This is situational, depending on the slope of N-factor versus x-location. Transition location is subject to more uncertainty at low Reynolds numbers than at high Reynolds numbers, due to the presumed spread in transition N-factor, since N-factor increases more quickly with x at high Reynolds numbers. Reference 54 tabulates this sensitivity about the measured transition location for HIFiRE-1 at various times. Transition x location sensitivity varies from $0.034 < \Delta x/\Delta N < 0.096$ (meters per unit N), for $19 < t < 22$ s. Taking into account nonlinearity in the N-factor versus x distribution, $8 < N < 15$ equates to an uncertainty of 35% of the cone length for HIFiRE-1 at t = 22 s.

Another concern regarding the assumed transition N-factor is the disturbance level, and variations thereof, in flight. Not enough hypersonic flight tests exist from which to develop a statistical sample of how flight disturbances affect transition. An N-factor of 14 (typical for HIFiRE-1 ascent transition) represents a million-fold amplification. This is not to say that the freestream disturbances were one-millionth of the boundary-layer disturbances at transition. Freestream disturbances had to be processed, presumably, through some receptivity process and some subsequent linear and nonlinear amplification. It suffices to say that initial disturbance levels were probably quite low, perhaps immeasurable, and small scale. The second mode wavelength at t = 22 s was on the order of several millimeters. Indeed, the ultimate source of flight disturbances is unknown, and may remain unknown. Bushnell speculated on numerous sources of initial disturbances.[57] Fedorov et al.[58] have calculated that thermal molecular fluctuations (Brownian motion) might have engendered transition on HIFiRE-1.

Since disturbances amplify so rapidly, changes in the initial disturbance field do not necessarily translate into large differences in the transition location, however. Assuming that a disturbance breaks down after one-million fold amplification (N = 13.8), another disturbance beginning at half the initial amplitude of the first, would have to undergo a two-million fold amplification (N = 14.5), assuming that the disturbances undergo the same amplification process and break down at the same amplitude. For HIFiRE-1 at t = 22 s, the difference between N = 13.8 and N = 14.5 equates to only a 67 mm difference in transition location.

Besides prediction of the absolute transition location, it appears that stability theory is well-suited to analyze parametric trends on HIFiRE-1-type configurations. During its period of second-mode transition, the HIFiRE-1 flight experienced only small parametric variations. Ground tests, however, covered a wider range of Mach number, Reynolds number and nose bluntness. Transition from two wind tunnels were well-correlated across the parameter

range by an N-factor of 5.5, over a range $6 < M < 10$ and nose bluntness from sharp to 6.35 mm radius. Later tests and analysis of similar configurations suggest that a variable N-factor for wind tunnel data that takes wind tunnel noise into account might be a better prediction method.[59] It should also be noted that a constant N-factor prediction method did not fare so well for correlating transition on HIFiRE-1 at AoA in ground tests.[11]

One goal of the HIFiRE experiments was to compare ground test transition to flight test transition. Figure 2 illustrates heat transfer data obtained in two wind tunnels and in flight. The flight time of $t = 22$ s was chosen since it was the lowest Reynolds number at which clean transition data was obtained, and thus closer to the wind tunnel Reynolds numbers. Data were normalized with edge conditions to minimize Mach number differences. The disparity between ground and flight test transition is evident.

Since the actual flight conditions varied from the preflight tests, it was not possible to make a one-to-one comparison among the wind tunnel tests and flight data. The wind tunnel tests were conducted at higher Mach numbers and with T_w/T_0 ratios different from the ascent transition conditions. Also, Reynolds numbers based on nose radius were different. By considering parametric trends, however, some conclusions may be derived. Figure 3 illustrates transition Reynolds numbers for the HIFiRE configuration as a function of the nose radius Reynolds number. Table 1 lists conditions for these tests. For comparison, and to illustrate the transition trend with nose radius, Stetson's 8° cone transition data[60] (replotted from Ref. 61) are included on the graph. Transition Reynolds numbers were normalized with edge conditions to minimize effects from differing Mach numbers and cone angles. Edge values were based on Taylor-Maccoll solutions for sharp cones.

Despite the variations in conditions, the HIFiRE -1 flight data clearly trend higher than the wind tunnel data. The HIFiRE flight transition Reynolds number in Figure 3 is about 1.4 times higher than the Stetson Mach 6 data trend, and about twice the data trend for the HIFiRE-specific geometry.

Another potential confounding factor in comparing the wind tunnel to flight data is differences in wall cooling. However, Table 1 shows that the wind tunnel tests possessed wall temperature ratios either equivalent to or higher than the flight data. Assuming that transition was due to second-mode instabilities for all cases, decreasing T_w/T_0 for ground test, or increasing T_w/T_0 for the flight test, would only accentuate the differences between flight and wind tunnel transition Reynolds numbers, due to the destabilizing effect of wall-cooling on the second mode.

The effect of noise is clearer when N-factors are compared. The N-factor computations should take parametric differences between the flight and ground test into account. The correlating N-factors of 5.5 derived from wind tunnel tests[11] compared to the N = 13-14 correlating values observed in flight clearly demonstrate the dominance of wind tunnel noise in ground test.

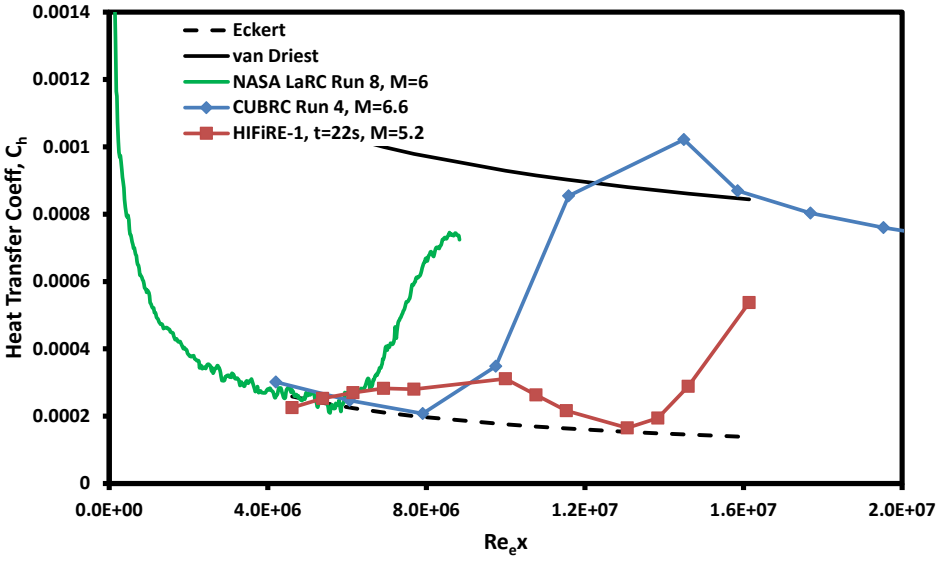

Figure 2 Heat transfer data from wind tunnel tests and flight.

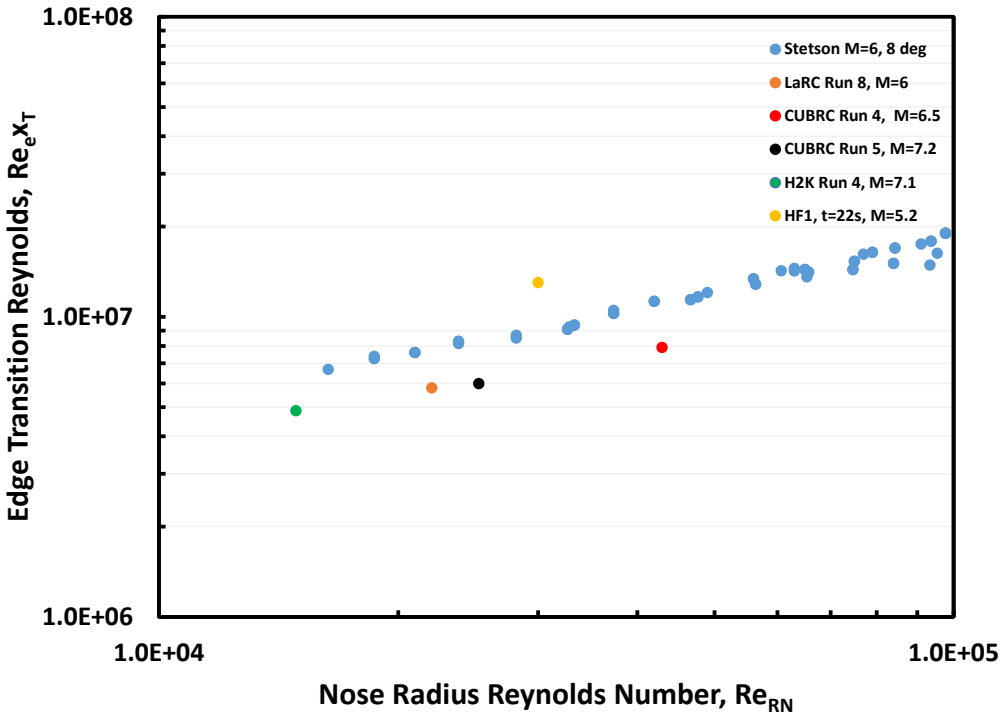

Figure 3 Transition Reynolds number based on edge conditions as function of nose radius Reynolds number.

Table 1 Ground Test Conditions.

	NASA Run 8	CUBRC Run 4	CUBRC Run 5	H2K Run 4	HIFiRE-1, t=22s	Stetson
M	6	6.6	7.2	7.1	5.2	6
Re/m	1.9E+07	1.7E+07	1.0E+07	9.3E+06	1.2E+07	var
Re_{RN}	22051	42968	25262	14880	30000	var
T_w/T_0	0.60	0.16	0.13	0.56	0.17	0.49

IV. Transition in Three-Dimensional Flows – HIFiRE-1 Experimental Data

Both HIFiRE-1 and -5b flights provided information on hypersonic flight transition in fully three-dimensional flows. HIFiRE-5, because of its spanwise pressure gradient, possessed cross-flow even at zero AoA. HIFiRE-1 attained cross-flow data inadvertently during descent, due to its AoA. Although the HIFiRE-1 flight was not intended to acquire data at nonzero AoA, it was recognized that this might occur. To mitigate this risk, instrumentation was selected with sufficient frequency response to resolve fluctuations in the transition front due to vehicle attitude variations.

The HIFiRE-1 descent transition front was mapped out by determining the angular location and Reynolds number at which each transducer registered transition, as the spinning payload descended. The transition history recorded by each transducer may be visualized by assuming that the spatially nonuniform transition front was wind-fixed, and the transducer revolved beneath it. Early in the descent, at low Reynolds number, a transducer would indicate laminar flow continuously. As the Reynolds number increased, a transducer would register periods of laminar and turbulent flow during each revolution of the payload, due to the spatially nonuniform transition front. Finally, the transducer would be completely downstream of the transition front, and register continuously turbulent flow at all azimuthal locations. The highest bandwidth instrumentation, the Vatell heat transfer gauges and Kulite pressure transducers, registered the transition front with the highest temporal fidelity. The Medtherm coaxial thermocouples showed some evidence of the transition front nonuniformity, but this was greatly smeared due to their lower frequency response.

Transition data obtained in this fashion are presented as a function of transducer azimuthal location, relative to the windward attachment line, and Reynolds number based on freestream conditions and x-location. Formally, this presentation resembles typical x-ϕ maps of transition, for example those generated by Stetson.[62] It must be noted that

HIFiRE-1 underwent significant variations in AoA and freestream Reynolds number over the region covered by this map. Nevertheless, this presentation of the data permits general features of the transition front to be compared to static wind tunnel data and CFD, and the conclusions derived from the data are not invalidated.

Figure 4 (from Ref. 17) illustrates the HIFiRE-1 transition front during descent, and the transition front measured in the DLR H2K wind tunnel.[63,64,65] Several notable features are apparent in this figure. First, data collected from three Kulite transducers (called out as "PHBW" in the figure), a Vatell heat transfer gauge ("HT3") and Medtherm coaxial gauges (dot-dash line, "Re_{TR}") are all consistent. Although the Medtherm gauges did not possess sufficient frequency response to resolve the transition front spatial nonuniformity, the transition location measured with the Medtherms falls at a Reynolds number that is the average transition Reynolds number observed with the higher bandwidth instruments.

Second, transition occurred at lower Reynolds numbers on the leeward centerline (Φ=180°), and higher Reynolds numbers on the attachment line (Φ=0°). This was expected and consistent with past wind tunnel results.[62-68,] A somewhat unexpected feature was that the highest transition Reynolds number occurred not on the windward or leeward symmetry meridians at Φ=0° and Φ=180°, but between them at about Φ=40° and Φ=300°. This multilobed transition front is probably the result of multiple transition processes, with traveling instabilities dominating transition on the windward and leeward meridians, and crossflow dominating between these meridians.

Third, the shape of the transition front measured in the H2K wind tunnel is somewhat similar to the shape of the flight transition front, with a low transition Reynolds number on the leeward meridian, and higher transition Reynolds number on the windward meridian. The H2K transition front does not appear to be sharply indented like the flight transition front, although the meager spatial resolution of the H2K measurements made this difficult to resolve.

Fourth, the leeward wind tunnel transition Reynolds numbers were lower than those measured in flight, as anticipated. Unexpectedly, however, wind tunnel transition on the windward meridian occurred at higher transition Reynolds numbers than in flight. Both this observation and the indented shape of the flight transition front are believed to be related to the higher wall-cooling of the flight article, as described below.

Various wind tunnel tests of smooth blunt cones, including the HIFiRE configuration itself, have shown contradictory trends of windward transition front movement with AoA. For HIFiRE-1 in H2K, the α=6° and α=12° windward transition Reynolds numbers (Re_x=5.3x10^6 and Re_x=6.4 x10^6, respectively) were higher than the α=0° transition Reynolds number (Re_x=3.9 x10^6), in contrast to the flight test trends. Similarly, tests of HIFiRE-1 in the NASA Langley Research Center (NASA LaRC) 20-Inch Mach 6 wind tunnel at α =0°, 3°, and 5° showed transition moving downstream on the windward meridian as AoA increased, although the change was modest.[14] Tests of HIFiRE-1 at Calspan University of Buffalo Research Center (CUBRC), however, displayed trends contrary to the H2K and LaRC tests. At α =0°, 1°, 2°, and 5°, and M= 6.6 and 7.2 in CUBRC, the windward transition front moved upstream with increasing AoA.[12] Some other wind tunnel tests have displayed upstream movement of the windward transition front with AoA on cones with small nose bluntness. In all of the ground test cases, leeward transition also moved upstream with increasing AoA, and thus remained upstream of windward transition, as it did in the HIFiRE flight results.

The nature of the disturbances, and their interaction with wind tunnel noise and wall temperature, offers a possible explanation for these observations. High-bandwidth pressure transducers in the H2K experiment showed a strong instability on the windward centerline consistent with a second-mode transition. Computations also predicted second-mode windward transition in flight.[54] Second-mode instability is affected by wind tunnel noise, creating a trend toward lower transition Reynolds numbers in ground test, all else being equal.[69] However, second-mode is destabilized by wall-cooling, and the flight vehicle wall was more highly cooled than in ground test. The ratio of wall-to-total-temperature, T_w/T_0, was 0.56 in the H2K test, compared to 0.18 in flight. It is possible that increased wall-cooling in the flight test more than compensated for lower noise in the flight environment, leading to lower windward transition Reynolds number in flight compared to ground test. Wall temperature ratio for the CUBRC tests, which showed upstream windward transition movement like the flight, was T_w/T_0 = 0.13, relatively close to the flight value of 0.18. Also, the indented transition front observed on HIFiRE-1 in flight has been observed in ground test on highly cooled models.[67, 68, 70, 71]

It should also be noted that for swept cylinders tested at Mach 3.5, wind tunnel noise did not appear to affect leading edge transition.[72] In analogy to the swept cylinder attachment line, the cone attachment line may exhibit a similar lack of sensitivity to wind tunnel noise.

The apparent lesser effect of wind tunnel noise on transition around the shoulders of the model (Φ=90° and 270° on HIFiRE-1) might also be explained by the presence of crossflow instabilities. The putative second-mode spectral peak observed on the windward centerline in the H2K test was less prominent, or in some cases absent, away from the windward meridian. Infrared images in H2K also showed streaks consistent with a crossflow-induced transition.

This evidence strongly suggests that transition on the shoulder of the model was crossflow-dominated. Since stationary crossflow instabilities are presumed to be less sensitive to wind tunnel noise, this might account for the lesser impact of wind tunnel noise on the shoulder transition in the H2K test, compared to zero AoA tests.

Wall-cooling is expected to stabilize stationary crossflow to a limited extent, but this effect is probably minimal. Gosse, for example, showed that wall-cooling reduced the crossflow Reynolds number on a sharp 2:1 elliptic cone at Mach 8.[73] The higher shoulder transition Reynolds numbers on the flight article, compared to wind tunnel tests, might thus be due in part to increased wall-cooling, as well as lower noise.

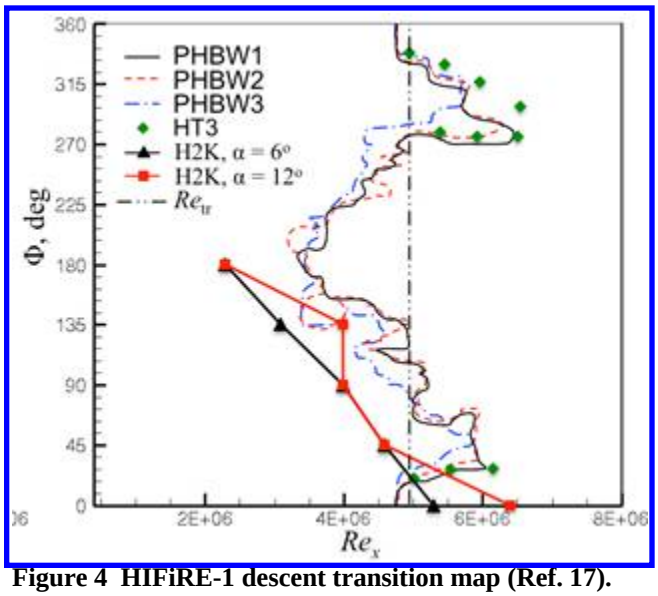

Figure 4 HIFiRE-1 descent transition map (Ref. 17).

V. Transition in Three-Dimensional Flows – HIFiRE-5 Experimental Data

Data analysis for HIFiRE-5 faced a challenge similar to HIFiRE-1, namely, merging transition records from multiple transducers at various times during descent. Similar to HIFiRE-1, transition events derived from all transducers were synthesized into maps of the transition location in ϕ - Reynolds space. Also, like HIFiRE-1, this meant that when each transition event was registered, the vehicle was at a different attitude. AoA was less than 1°, and the vehicle attitude did not have a major impact on transition Reynolds number on the centerline and leading edge meridians. At the maximum crossflow location, near the shoulder of the model (ϕ =45° on HIFiRE-5), however, transition was quite sensitive to yaw angle. Transition at the shoulder of the test article was promoted when that side was yawed into the wind. Therefore, some transducers registered multiple transition and laminarization events before they recorded continuously turbulent flow. The detailed effect of vehicle yaw is reserved for future analysis. The transition data presented in this section are based on first departure of a transducer from laminar heating. Therefore, they represent a transition Reynolds number for the most unstable attitude for that transducer.

Figure 5 (from Ref 21) shows flight transition Reynolds number as a function of spanwise location, at three different *x*-stations. This figure clearly shows three transitional lobes emanating from (top-to-bottom in the figure) leading edge, shoulder (ϕ = 45°) and centerline. Undoubtedly, multiple instabilities led to this multi-lobed transition front. The transition pattern is similar at each *x*-station. For each of the lobes, the transition Reynolds number varied less than 10% with streamwise location. In the two regions of delayed transition (centered near ϕ =25° and 70°), the transition Reynolds number and the azimuthal location of maximum transition Reynolds number was more variable. As discussed above, the transition Reynolds numbers in Figure 5 near the ϕ =45° region are more representative of the condition where that side is yawed into the wind.

At present, there is no wind tunnel test directly replicating flight conditions. Several wind tunnel tests of HIFiRE-5 exist at Mach 6 and 7, and for a sharp 2:1 elliptic cone at M = 8. HIFiRE-5 was tested at Purdue University, under quiet and noisy flow conditions, and at NASA LaRC, under noisy flow. The Purdue and LaRC tests used identically-scaled models. The sharp 2:1 elliptic cone was tested at M=8 under noisy conditions in Tunnel B of the Arnold Engineering Complex von Karman Facility (AEDC VKF-B). Limited qualitative infrared imaging data were obtained at M =7 at CUBRC.

The most comprehensive wind tunnel data were obtained in the Purdue Mach 6 quiet tunnel. Data included oil flows, temperature-sensitive paint, infrared imaging, and Kulite and PCB surface pressure measurements under noisy and quiet conditions. These tests displayed stationary crossflow instabilities under quiet flow with oil flow, temperature-sensitive paint and IR.[29-31, 33-35, 39] Figure 6 (from Ref. 34) illustrates the heat transfer signature of stationary crossflow vortices and transition in the Purdue wind tunnel at M=6 and Re=12.3×10^6 /m under quiet flow. Stationary crossflow instabilities were only weakly evident under noisy flow. Traveling crossflow instabilities were measured in quiet flow, but could not be observed under noisy conditions. Kulite pressure transducer arrays permitted extraction of wave angle and phase velocity from traveling crossflow instabilities in quiet flow. Centerline and acreage transition was observed under both quiet and noisy conditions. The Purdue tunnel could not achieve a high-enough Reynolds number to produce leading edge transition under either noisy or quiet flow. Transition under quiet flow consisted of multiple lobes, with transition appearing most upstream on the centerline and the shoulder of the model. The lobe structure of the transition front was less well-defined under noisy flow, as discussed below.

Tests of HIFiRE-5 at LaRC under noisy flow focused on thermographic phosphor imagery.[24, 36, 38] Noisy transition data were obtained for all locations on the model, from centerline to leading-edge, including data with sideslip and angle of attack. Testing at the Texas A&M University Actively-Controlled-Expansion wind tunnel explored wind tunnel noise effects.[32] Later testing in this tunnel showed transition patterns similar to those obtained in the Purdue tunnel, and evidence for stationary crossflow vortices.[74]

Figure 7 compares flight and wind tunnel transition. Most of the ground tests did not replicate flight T_w/T_0, which is suspected to be a significant difference, especially for the attachment line transition. Tests at CUBRC more nearly matched flight wall-cooling. Wall-cooling destabilizes second-mode instabilities, but reduces crossflow Reynolds number.[73] Despite the dissimilarities among these tests and flight conditions, some general conclusions may be drawn regarding HIFiRE-5 transition in the wind tunnel versus flight.

First, the centerline transition occurred at a relatively low Reynolds number in flight, as it did in ground test. The centerline transition was dominated by the strongly inflected velocity profile here, making the boundary-layer susceptible to rapidly-amplifying traveling instabilities. The scenario is probably similar to leeside transition on HIFiRE-1 at AoA. HIFIRE-5 flight centerline transition occurred at Re_x~4.5x10^6 at Mach 7.8. HIFiRE-1 leeward transition occurred at Re_x~3.2x10^6 at Mach 7.0. This is contrasted with HIFiRE-1 zero AoA transition at M=5.3, which took place at $Re_x \sim 10^7$.

Second, for the wind tunnel cases, centerline transition under noisy flow occurred at much lower Reynolds numbers (about 1x10^6) than in flight (approximately 4.5x10^6). In quiet flow, centerline transition occurred at a Reynolds number of about 3.2x10^6, much closer to the flight value. This transition Reynolds number decrement due to tunnel noise, a factor of approximately 3, is comparable to that seen for HIFiRE-1 at α=0° and $M \sim 5.2$. Multiple centerline transition points for the LaRC data represent different unit Reynolds number cases, with higher transition Reynolds number corresponding to higher unit Reynolds number. This effect is often attributed to the spectral distribution of wind tunnel noise.[59]

Third, the distinct lobe near ϕ=45° that was present in flight and quiet wind tunnel flow was still evident in noisy flow. Linear stability calculations and wind tunnel tests indicated that transition near ϕ =45° was crossflow-dominated. TSP and IR imaging show that crossflow transition in the Purdue tunnel slightly preceded near-centerline transition in quiet flow, but under noisy flow, this was reversed, and near-centerline transition preceded crossflow transition. This earlier transition and lateral spreading of the near-centerline transition apparently made the transition-front indentation occurring near ϕ=25° in quiet flow somewhat less prominent in noisy flow. The LaRC noisy tests also showed a transitional lobe near ϕ=45°. Figure 8 presents a thermographic phosphor image demonstrating this structure. Although a lobed structure was present in these images, the inboard portion of the transitional lobe was difficult to resolve from numerical heat transfer data, so Figure 7 shows only the outboard portion of the lobe for the LaRC data. The plot of the LaRC data incorporates both left and right sides of the model, creating some scatter due to left/right asymmetry in the transition front. Although there is little overlap in the LaRC and the Purdue noisy data, the two data sets appear consistent. For comparison, Figure 9 shows heating contours obtained under noisy flow in the Purdue wind tunnel at conditions similar to those of the LaRC data in Figure 8. Since the Purdue and LaRC models were the same size, the similarity in the transition fronts is readily apparent.

The observation that wind tunnel noise affected near-centerline transition, which was dominated by traveling instabilities, slightly more than the crossflow transition, is consistent with the supposition that wind tunnel noise would affect traveling instabilities more strongly than stationary instabilities. That wind tunnel noise had this impact on crossflow transition is somewhat surprising, given the presence of stationary crossflow in this region. Traveling disturbances must develop somehow during the crossflow transition process however, as energy at zero frequency is distributed to nonzero frequencies, and wind tunnel noise may impact this process. Also, traveling crossflow waves

were observed prior to transition in quiet flow, although the relative roles of traveling and stationary crossflow instability remains unclear.[33]

A fourth observation is that the flight case shows a distinct leading-edge transition lobe. Leading edge transition occurred in the LaRC tests, but it appeared to have a different character. Transition occurred on the leading edge, but it was the most downstream transition location on the model. Similar leading edge transition behavior occurred on the sharp elliptic cone at M=8.[48] In noisy flow, leading edge transition perhaps arose from spanwise contamination from adjacent turbulent regions. Even so, wind tunnel noise did not seem to affect outboard ($\phi > 50°$) and leading edge transition as radically as centerline transition. In the LaRC tests, leading edge transition occurred at $Re_x \sim 3.7 \times 10^6$, compared to about 4.5×10^6 in free flight. This result is somewhat reminiscent of the behavior of the HIFiRE-1 windward side transition when that test article was at angle of attack. In this case, windward transition Reynolds numbers in noisy flow were comparable to or even exceeded flight transition Reynolds numbers. At least part of this difference was ascribed to the higher wall cooling on the flight vehicle.[17]

The exception to these ground-test results for leading edge transition was the temperature-sensitive paint images obtained at CUBRC at about M=7.[26] In this study, at least one image seemed to show a leading edge transition lobe where transition occurred at Reynolds numbers nearly identical to or lower than centerline transition.

That the multi-lobed transition front was observed both in flight and in the quiet wind tunnel, and that the same trends in crossflow transition were observed in wind tunnel and flight, is a powerful indication that the quiet tunnel accurately represented the flight transition mechanism. This further reinforces the notion that the flight transition was the result of modal instabilities, as observed in the wind tunnel.

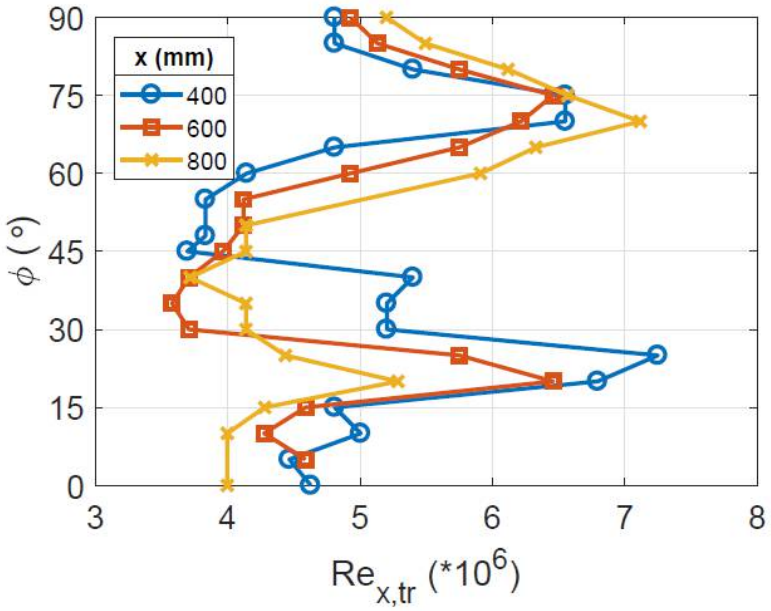

Figure 5 Transition Reynolds numbers at three streamwise locations (Ref 21).

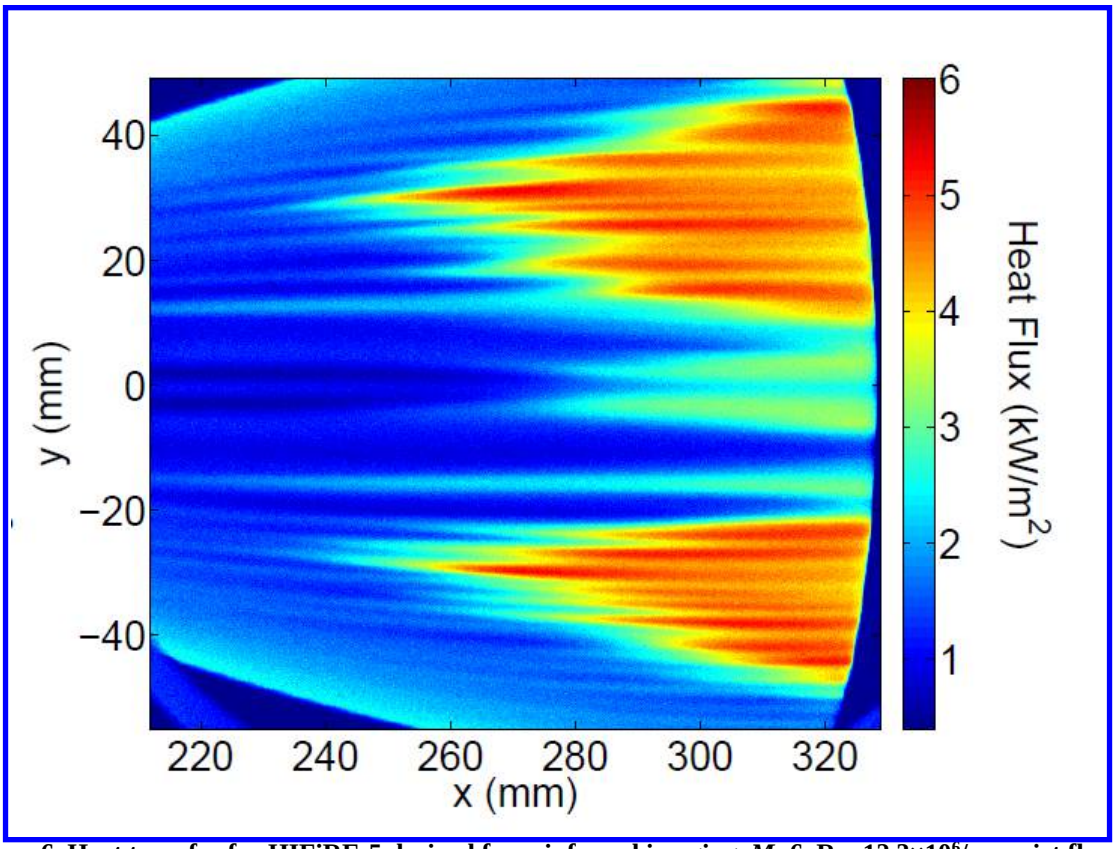

Figure 6 Heat transfer for HIFiRE-5 derived from infrared imaging, M=6, Re=12.3×10^6/m, quiet flow, Purdue wind tunnel (Ref. 34).

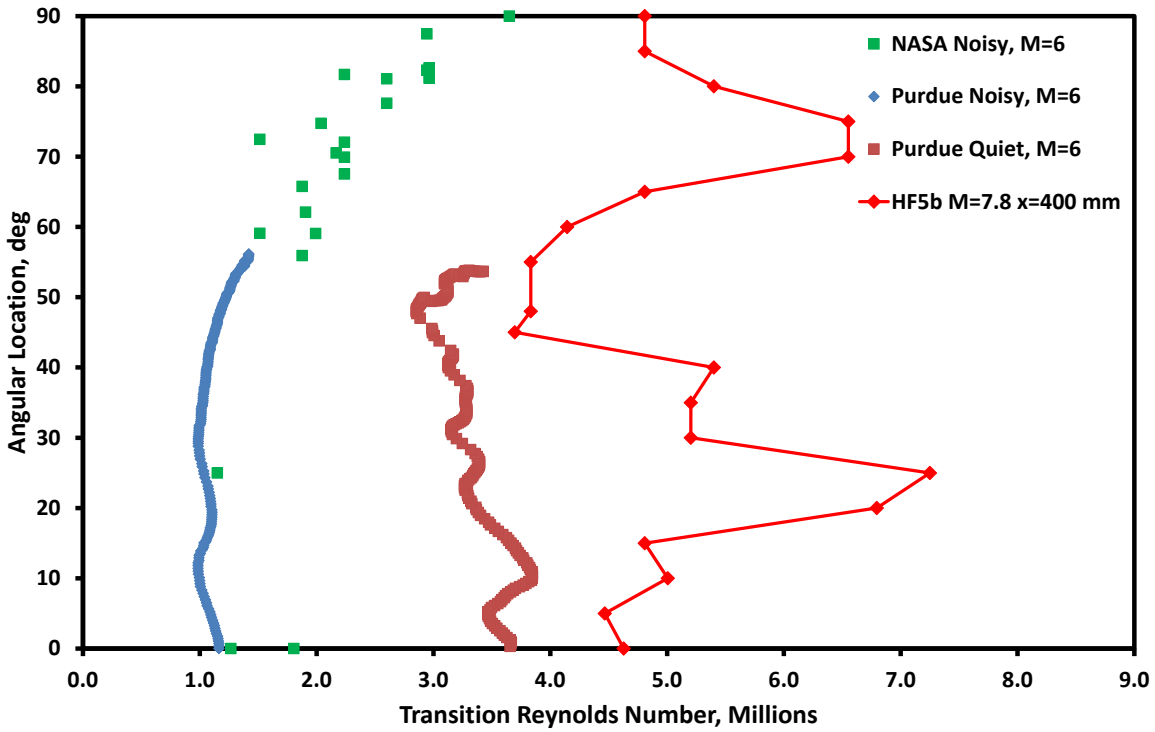

Figure 7 Noisy and quiet wind tunnel transition compared to flight transition.

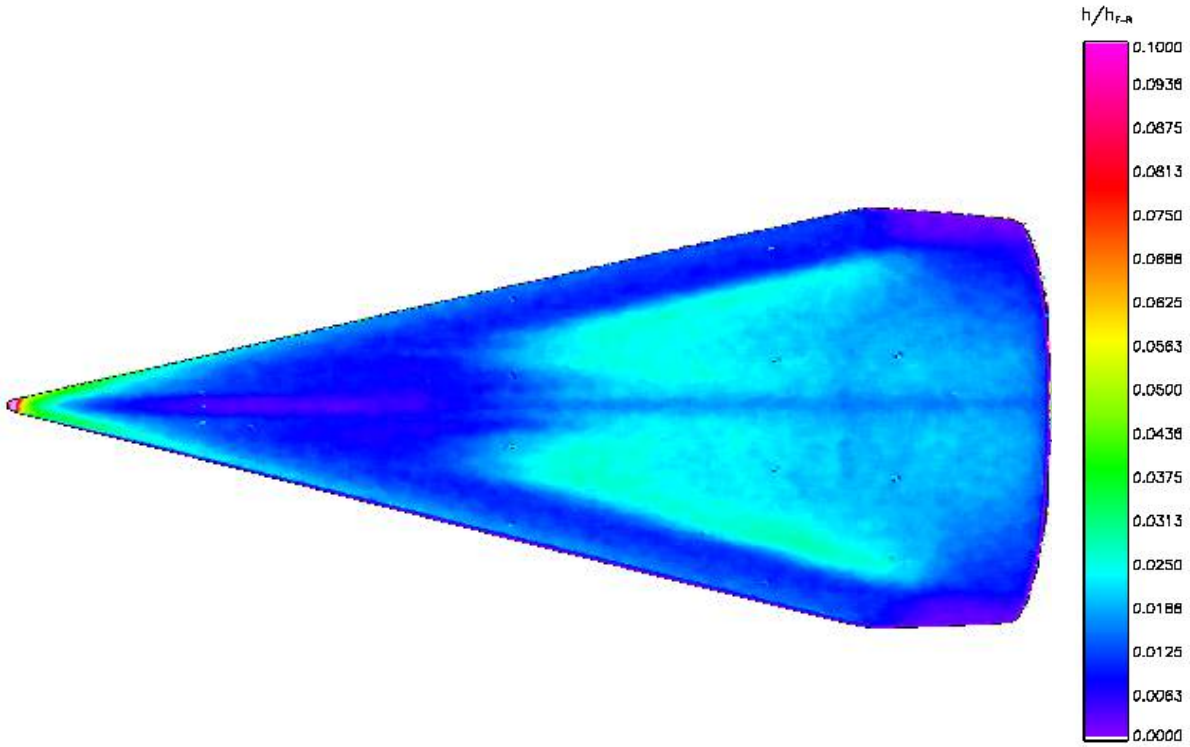

Figure 8 Heat transfer contours derived from thermographic phosphor image from LaRC Run 8. M=6, Re=9.5×10^6 /m, α=0°. Enlarged image extracted from Ref. 36.

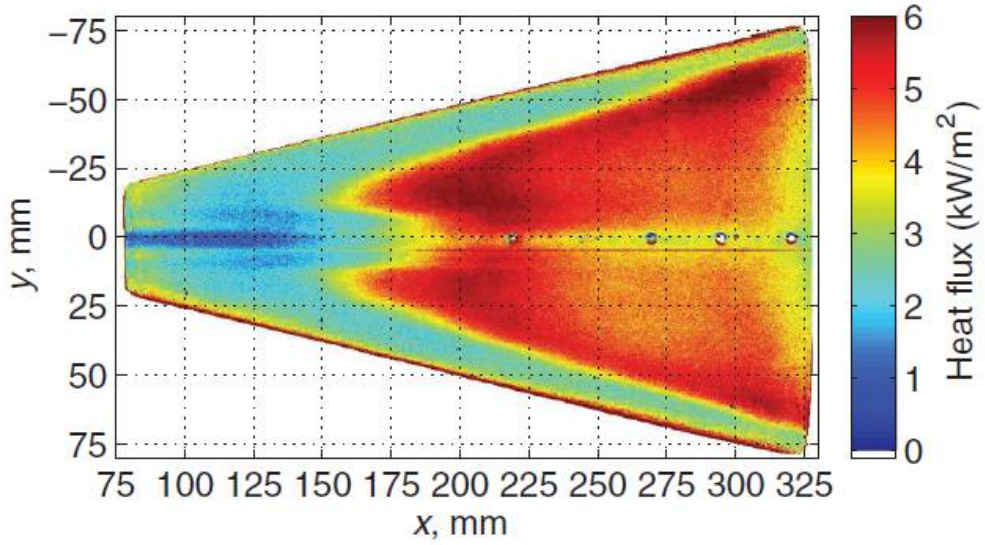

Figure 9 Heat transfer contours derived from temperature-sensitive paint image from Purdue wind tunnel M=6, Re=10.2×10^6 /m, α=0°, noisy flow (Ref. 39).

VI. Transition in Three-Dimensional Flows – HIFiRE-1 and -5 Computations

Boundary-layer stability calculations for HIFiRE-1 at angle of attack were generally successful in replicating flight transition phenomenology. Li et al.[75] executed post-flight stability calculations for several points in the descent trajectory, labeled R1-R4, with increasing time (Table 2). Each point represented a significant event. R1 (t = 481.3s) corresponded to a condition with fully laminar flow, but with periodic pressure fluctuations near the shoulder of the test article. These pressure fluctuations peaked at condition R2 (t = 483.7 s). Conditions R3 and R4 were for the same time (t = 485 s), but different angles of attack (α = 7.5° and 6.1° respectively). At conditions R3 and R4, flow had just become fully turbulent at all azimuthal locations at the x=850 mm, where most of the high bandwidth instrumentation was clustered.

Parabolized Stability Equation (PSE) calculations for R1 predicted a maximum N-factor on the windward centerline of 6.4, consistent with the laminar flow observed in flight at this time. For point R2, the N-factor at x=850 mm was 14, consistent with the first appearance of transition in flight on the windward centerline at t = 483.8 s. For condition R4, the N-factor at x = 850 mm exceeded 14, consistent the observation of turbulent flow in flight at this time. Interestingly, the N-factor at the aft-most portion of the test article was 23 on the windward meridian, but only 9.5 on the leeward meridian. Li et al.[75] attributed the relatively slow instability growth on the leeward meridian to the structure of the mean flow there.

No attempt was made to develop a correlating N-factor for crossflow transition in flight, but the computational observations were broadly consistent with flight observations. Stationary crossflow calculations indicated an N-factor of 9.5-10 at x = 850 mm for condition R1, which was shortly before flow at the shoulder of the test article became turbulent at this station. For condition R4, crossflow N-factors exceeding 14 were predicted for x = 850 mm, with N-factors attaining a value of 23 at the end of the cone. These results were consistent with observations of fully laminar flow in flight at condition R1, and fully turbulent at R4.

Tufts executed post-flight linear PSE computations for HIFiRE-5, examining leading edge and crossflow stability. N-factor contours presented a lobed appearance similar to the transition front data. Traveling instabilities dominated the leading edge, and crossflow instability dominated the acreage. By comparing the computed N-factors to flight transition data, Tufts estimated the N-factors at transition on the acreage and leading edge to be 10 and 18, respectively. The acreage flight transition data were affected by model yaw angle, however, so the N=10 value is probably more indicative of conditions where that side of the model was yawed into the wind.

Tufts also executed PSE computations for some post-flight wind tunnel cases. Again, computed N-factor contours resembled the transitional lobes displayed in the wind tunnel tests. The N-factor of 10 that correlated the flight crossflow transition also appeared to correlate wind tunnel crossflow transition. Movement of the N=10 contour with AoA also resembled the transition front movement observed in the wind tunnel with AoA. Moyes, et al.[76] also using linear PSE, determined crossflow N-factors at transition of 5-8 for flight.

Choudhari et al. performed pre-flight stability calculations for HIFiRE-5 at anticipated flight conditions. These calculations included computations of centerline instabilities, as well as attachment line and crossflow. Notably, these computations indicated a strongly unstable leading edge, with N-factors similar to the unstable centerline boundary-layer. Given that the leading edge transition in flight occurred at nearly the same Reynolds number as the centerline transition, it seems plausible that the computed stability behavior on these meridians accurately represented flight.

Despite the high amplification predicted for the leading edge in flight, uncontaminated leading edge transition was observed only in CUBRC, where the ratio of wall to stagnation temperature was closer to the flight test. In analogy to the attachment line flow on the cone at angle of attack, it is suspected that cooling is highly destabilizing to the HIFiRE-5 leading edge.

Table 2 HIFiRE-1 Descent Analysis Cases.

Case	Time (s)	α (deg)
R1	481.3	13.6
R2	483.7	9.6
R3	485.0	7.5
R4	485.0	6.7

VII. Conclusions

Perhaps the most significant conclusion from the HIFiRE-1 and -5 research campaigns was the success of boundary-layer stability theory in reproducing transition trends and patterns, implying that the stability calculations

and wind tunnel tests reproduced at least some of the transition physics observed in flight. Although boundary-layer instabilities were not directly measured in flight, the correlation between flight transition trends and those observed in ground test and computation is persuasive evidence that modal instabilities were responsible for transition in flight. This is not a trivial conclusion. Given the small scale and high frequency expected for these instabilities, it was not clear that the flight environment would provide sufficient excitation to generate them. Although *N*-factor correlations and ground test were able to replicate some trends from prior hypersonic flight tests, these predictions may have merely been simulants for some other, undetermined, instability process that occurred in flight. We can now proceed with greater confidence to apply these tools to flight. Although these tools suffer recognized limits, they appear applicable to a wide range of flow scenarios.

The goal of using the HIFiRE flights to calibrate *N*-factor predictions and ground test was achieved, within the limits of the *N*-factor transition prediction approach. It is probably unrealistic to expect a single *N*-factor to correlate transition across a broad range of scenarios. Linear growth represents only a portion of the stability process. Variations in initial amplitudes, receptivity and nonlinear amplification probably all affect the best correlating *N*-factor. However, given the relatively high transition *N*-factors attained by the HIFiRE flights, the HIFiRE flight transition *N*-factors probably represent near-upper limits on attainable *N*-factors for smooth bodies. Since flight conditions, including disturbance levels and vehicle roughness, may vary from flight-to-flight, a statistical approach to transition prediction is probably warranted.

The subsidiary goal of calibrating ground test transition Reynolds numbers to flight was partially successful. In analogy to calibrating *N*-factor predictions, this goal was probably somewhat unrealistic, given the myriad parametric effects possible in ground test. This might be rectified in some cases by repeating ground tests with conditions tailored to flight. Despite this, some general conclusions could be reached. Axisymmetric, leeward and crossflow transition all showed lower transition Reynolds numbers or *N*-factors in the wind tunnel compared to flight. The impact of noise on HIFiRE-5 leading edge transition was not as great as for the other transition scenarios. Windward attachment line transition was an even more dramatic exception. HIFiRE-1 windward transition actually occurred at a lower Reynolds number in flight compared to the wind tunnel. The implication from this observation is that either attachment line transition is not as severely impacted by wind tunnel noise as the other transition mechanisms, or it is exceptionally sensitive to wall temperature differences. For attachment lines, the wind tunnel transition may not represent a "worst case" scenario, and designers should exercise due caution.

Acknowledgments

A very large number of organizations and people contributed to the HIFiRE-1 and -5 research programs. The authors wish to thank the AFRL Aerospace Systems Directorate and its precursor organizations, and Ivett Leyva and her predecessors at the Air Force Office of Scientific Research, including John Schmisseur and Pon Ponnapan for their sponsorship. Douglas Dolvin of the AFRL Aerospace Systems Directorate provided program management. Flight tests were executed by the Air Vehicles Division, Brisbane, of the Defence Science and Technology Organisation and the Defence Science and Technology Group, Royal Australia Navy Ranges and Assessing Unit, Aerospace Operational Support Group, Royal Australian Air Force, White Sands Missile Range, DTI/Kratos, and DLR Moraba. Ground test support and analysis was provided by the NASA Langley Research Center, Purdue University, Texas A&M University and CUBRC. Many individuals, too numerous to mention, provided valuable advice and feedback.

References

[1] Dolvin, D. "Hypersonic International Flight Research and Experimentation (HIFiRE) Fundamental Science and Technology Development Strategy," AIAA Paper 2008-2581, April 2008.

[2] Dolvin, D. J., "Hypersonic International Flight Research and Experimentation Technology Development and Flight Certification Strategy," AIAA paper 2009-7228, October 2009.

[3] Kimmel, R. L., Adamczak, D., Gaitonde, D., Rougeux, A., Hayes, J. R., "HIFiRE-1 Boundary Layer Transition Experiment Design," AIAA paper 2007-0534, January 2007.

[4] Wadhams, T. P., MacLean, M. G., Holden, M.S., and Mundy, E., "Pre-Flight Ground Testing of the Full-Scale FRESH FX-1 at Fully Duplicated Flight Conditions," AIAA paper 2007-4488, June 2007.

[5] Johnson, H. B., Alba, C. R., Candler, G. V., MacLean, M., Wadhams, T, and Holden, M. "Boundary Layer Stability Analysis of the Hypersonic International Flight Research Transition Experiments," *AIAA Journal of Spacecraft and Rockets*, vol. 45, no. 2, March-April 2008, pp. 228-236.

[6] Holden, M. S., Wadhams, T. P., MacLean, M., "Experimental Studies in the LENS Supersonic and Hypersonic Tunnels for Hypervelocity Vehicle Performance and Code Validation," AIAA paper 2008-2505, April 2008.

[7] Kimmel, R. L., "Aerothermal Design for the HIFiRE-1 Flight Vehicle," AIAA paper 2008-4034, June 2008.
[8] Casper, K. M., Wheaton, B. M., Johnson, H. B., and Schneider, S. P., "Effect of Freestream Noise on Roughness-Induced Transition at Mach 6," AIAA paper 2008-4291 June 2008.
[9] Casper, K. M., Johnson, H. B., and Schneider, S. P., "Effect of Freestream Noise on Roughness-Induced Transition for a Slender Cone," *AIAA Journal of Spacecraft and Rockets*, vol. 48, no. 3, May-June 2011, pp 406-413.
[10] Kimmel, R. L., "Roughness Considerations for the HIFiRE-1 Vehicle," AIAA Paper 2008-4293, June 2008.
[11] Alba, C. R., Johnson, H. B., Bartkowicz, M. D., Candler, G. V., and Berger, K. T. "Boundary-Layer Stability Calculations for the HIFiRE-1 Transition Experiment," *AIAA Journal of Spacecraft and Rockets*, vol. 45, no. 6, November-December 2008, pp. 1125-1133.
[12] Wadhams, T. P., Mundy, E., MacLean, M. G., and Holden, M. S., "Ground Test Studies of the HIFiRE-1 Transition Experiment Part1: Experimental Results," *AIAA Journal of Spacecraft and Rockets*, vol. 45, no. 6, November-December 2008, pp. 1134-1148.
[13] MacLean, M., Wadhams, T., Holden, M., and Johnson, H., "Ground Test Studies of the HIFiRE-1 Transition Experiment Part 2: Computational Analysis," *AIAA Journal of Spacecraft and Rockets*, vol. 45, no. 6, November-December 2008, pp. 1149-1164.
[14] Berger, K. T., Greene, F. A., Kimmel, R. L., Alba, C., and Johnson, H., "Erratum on Aerothermodynamic Testing and Boundary-Layer Trip Sizing of the HIFiRE Flight 1 Vehicle," *AIAA Journal of Spacecraft and Rockets*, vol. 46, no., 2, March-April, 2009, pp. 473-480.
[15] Adamczak, D., Alesi, H., Frost, M., "HIFiRE-1: Payload Design, Manufacture, Ground Test, and Lessons Learned," AIAA paper 2009-7294, October 2009.
[16] Kimmel, R. L., Adamczak, D., Paull, A., Paull, R., Shannon, J., Pietsch, R., Frost, M., and Alesi, H., "HIFiRE-1 Ascent-Phase Boundary-Layer Transition," *AIAA Journal of Spacecraft and Rockets*, vol. 52, no. 1, Jan-Feb 2015, pp 217-230.
[17] Stanfield, S. A., Kimmel, R. L., Adamczak, D. and Juliano, T. J., "HIFiRE-1 Data Analysis: Boundary Layer Transition Experiment During Reentry," *AIAA Journal of Spacecraft and Rockets*, vol. 52, no. 3, May-June 2015, pp 637-649.
[18] Kimmel, R. L., Adamczak, D. A., and DSTG AVD Brisbane Team, "HIFiRE-5b Flight Overview," AIAA paper 2017-3131, June 2017.
[19] Porter, K. M., Poggie, J., and Kimmel, R. L., "Laminar and Turbulent Flow Calculations for the HIFiRE-5b Flight Test," AIAA paper 2017-3132, June 2017.
[20] Jewell, J. S., Kimmel, R. L., Poggie, J., Porter, K. M., and Juliano, T. J., "Correlation of HIFiRE-5b Flight Data With Computed Pressure and Heat Transfer for Attitude Determination," AIAA paper 2017-3133, June 2017.
[21] Juliano, T., Poggie, J., Porter, K., Jewell, J., Kimmel, R.L., Adamczak, D. A., "HIFiRE-5B Heat Flux and Boundary-Layer Transition," AIAA paper 2017-3134, June 2017.
[22] Borg, M. and Kimmel, R. L., "Ground Test Measurements of Boundary-Layer Instabilities and Transition for HIFiRE-5 at Flight-Relevant Attitudes," AIAA paper 2017-3135, June 2017.
[23] Tufts, M. P., Gosse, R., and Kimmel, R. L., "PSE Analysis of Crossflow Instability on HIFiRE 5b Flight Test," AIAA paper 2017-0764, January 2017.
[24] Choudhari, M., Chang, C.-L., Jentink, T., Li, F., Berger, K., Candler, G., and Kimmel, R., "Transition Analysis for the HIFiRE-5 Vehicle," AIAA paper 2009-4056, June 2009.
[25] Gosse, R., Kimmel, R., and Johnson, H. B., "Study of Boundary-Layer Transition on Hypersonic International Flight Research Experimentation 5," *AIAA Journal of Spacecraft and Rockets*, vol. 51, no. 1, January 2014, pp 151-162.
[26] Juliano, T. J., Schneider, S., "Instability and Transition on the HIFiRE-5 in a Mach 6 Quiet Tunnel," AIAA paper 2010-5004, June 2010.
[27] Juliano, T. J., "Instability and Transition on the Hifire-5 in A Mach-6 Quiet Tunnel," Ph.D. Dissertation, Purdue University, West Lafayette, IN, August 2010.
[28] Holden, M. S., Wadhams, T. P., MacLean, M., Mundy, E., "Review of Studies of Boundary Layer Transition in Hypersonic Flows Over Axisymmetric And Elliptic Cones Conducted in the CUBRC Shock Tunnels," AIAA paper 2009-0782, January 2009.
[29] Borg, M., Kimmel, R. L., and Stanfield, S., "Instability and Transition for HIFiRE-5 in a Hypersonic Quiet Wind Tunnel," 2011-3247, June 2011.
[30] Borg, M. P., Kimmel, R. L., Stanfield, S., "Crossflow Instability for HIFiRE-5 in a Quiet Hypersonic Wind Tunnel," AIAA paper 2012-2821, June 2012.

[31] Borg, M. P., Kimmel, R. L., and Stanfield, S., "Traveling Crossflow Instability for HIFiRE-5 in a Quiet Hypersonic Wind Tunnel," AIAA 2013-2737, June 2013.
[32] Borg, M. P., Kimmel, R. L., Hofferth, J. W., Bowersox, R. D., and Mai, C. L., "Freestream Effects on Boundary Layer Disturbances for HIFiRE-5," Paper 2015-0278, AIAA, January 2015.
[33] Borg, M. P., and Kimmel, R. L., "Traveling Crossflow Instability for the HIFiRE-5 Elliptic Cone," *AIAA Journal of Spacecraft and Rockets*, vol. 52, no. 3, May-June 2015, pp. 664-673.
[34] Borg, M.P., and Kimmel, R. L., "Simultaneous Infrared and Pressure Measurements of Crossflow Instability Modes for HIFiRE-5," AIAA paper 2016-0354, January 2016.
[35] Borg, M. P., and Kimmel, R. L., "Measurements of Crossflow Instability Modes for HIFiRE-5 at Angle of Attack," AIAA paper 2017-1681, January 2017.
[36] Berger, K. T., Rufer, S. J., Kimmel, R. and Adamczak, D., "Aerothermodynamic Characteristics of Boundary Layer Transition and Trip Effectiveness of the HIFiRE Flight 5 Vehicle," AIAA paper 2009-4055, June 2009.
[37] Lakebrink, M. T., Borg, M. P., "Traveling Crossflow Wave Predictions on the HIFiRE-5 at Mach 6: Stability Analysis vs. Quiet Tunnel Data," AIAA paper 2016-0356, January 2016.
[38] Kimmel, R. L, Adamczak, D., Berger, K., and Choudhari, M., "HIFiRE-5 Flight Vehicle Design," AIAA paper 2010-4985, June 2010.
[39] Juliano, T. J., Borg, M. P. and Schneider, S. P., "Quiet Tunnel Measurements of HIFiRE-5 Boundary-Layer Transition," *AIAA Journal*, vol. 53, no. 4, April 2015, pp.832-846.
[40] Dinzl, D. J. and Candler, G. V., "Direct Simulation of Hypersonic Crossflow Instability on an Elliptic Cone," *AIAA J.*, vol. 55, no. 6, June 2017, pp. 1769-1782.
[41] Kimmel, R. L., Adamczak, D., Juliano, T. J., DSTO AVD Brisbane Team, "HIFiRE-5 Flight Test Preliminary Results," AIAA paper 2013-0377, January 2013.
[42] Juliano, T. J., Adamczak, D. and Kimmel, R. L., "HIFiRE-5 Flight Test Heating Analysis," AIAA paper 2014-0076, January 2014.
[43] Jewell, J. S., Miller, J. H., Kimmel, R. L., "Correlation of HIFiRE-5 Flight Data With Computed Pressure and Heat Transfer," AIAA paper 2015-2019, June 2015.
[44] Juliano, T. J., Adamczak, D., and Kimmel, R. L., "HIFiRE-5 Flight Test Results," *AIAA Journal of Spacecraft and Rockets*, vol. 52, no. 3, 2015, pp. 650-663.
[45] Schneider, S. P., "Flight Data for Boundary-Layer Transition at Hypersonic and Supersonic Speeds," *AIAA Journal of Spacecraft and Rockets*, vol. 36, no. 1, January-February 1999, pp 8-20.
[46] Kimmel, R. L., and Poggie, J., "Transition on an Elliptic Cone at Mach 8," American Society of Mechanical Engineers ASME FEDSM97-3111, June 1997.
[47] Kimmel, R. L., and Poggie, J., "Three-Dimensional Hypersonic Boundary Layer Stability and Transition," Air Force Research Laboratory Technical Report, WL-TR-97-3111, December 1997, Wright-Patterson Air Force Base, Ohio.
[48] Kimmel, R. L., and Poggie, J., Schwoerke, S. N., "Laminar-Turbulent Transition in a Mach 8 Elliptic Cone Flow," *AIAA Journal*, vol. 37, no. 9, Sep. 1999, pp. 1080-1087.
[49] Schmisseur, J. D., "Receptivity of the Boundary Layer on a Mach-4 Elliptic Cone to Laser-Generated Localized Freestream Perturbations," Doctoral Dissertation, Purdue University Aerospace Sciences Laboratory, December 1997.
[50] Holden, M., "Experimental Studies of Laminar, Transitional, and Turbulent Hypersonic Flows Over Elliptic Cones at Angle of Attack," Air Force Office of Scientific Research Technical Report AFRL-SR-BL-TR-98-0142, Bolling Air Force Base, DC, 1998.
[51] Schmisseur, J. D., Schneider, S. P., and Collicott, S. H., "Receptivity of the Mach 4 Boundary Layer on an Elliptic Cone to Laser-Generated Localized Freestream Perturbations," AIAA paper 1998-0532, January 1998.
[52] Schmisseur, J. D., Schneider, S. P., and Collicott, S. H., "Response of the Mach 4 boundary layer on an elliptic cone to laser-generated freestream perturbations," AIAA paper 1999-0410, January 1999.
[53] Lyttle, I. J., and Reed, H. L., "Use of Transition Correlations for Three-Dimensional Boundary Layers Within Hypersonic Flows," AIAA-95-2293, June 1995.
[54] Li, F., Choudhari, M., Chang, C.-L., Kimmel, R., Adamczak, D., and Smith, M., "Transition Analysis for the Ascent Phase of HIFiRE-1 Flight Experiment," *AIAA Journal of Spacecraft and Rockets*, vol. 52, no. 5, September-October 2015, pp. 1283-1293.
[55] Johnson, H. B., and Candler, G. V., "PSE Analysis of Reacting Hypersonic Boundary Layer Transition," AIAA paper 99-3793, June 1999.
[56] Malik, M. R., "Hypersonic Flight Transition Data Analysis Using Parabolized Stability Equations with Chemistry Effects," *AIAA Journal of Spacecraft and Rockets*, Vol. 40, No. 3, May-June 2003, pp 332-344.

[57] Bushnell, D., "Notes on Initial Disturbances Fields for the Transition Problem," *Instability and Transition*, Vol. 1, edited by M. Y. Hussaini, and R. G. Voigt, Springer–Verlag, Berlin, 1990, pp. 217–232.
[58] Fedorov, A. and Tumin, A., "Receptivity of High-Speed Boundary Layers to Kinetic Fluctuations, *AIAA Journal*, vol. 55, no. 7, July, 2017, pp. 2335-2348.
[59] Marineau, E. C., "Prediction Methodology for 2nd Mode Dominated Boundary Layer Transition in Hypersonic Wind Tunnels," *AIAA Journal*, vol. 55, no. 2, Feb. 2017, pp. 484-499.
[60] Stetson, K. F., Thompson, E. R., Donaldson, J. C., and Siler, L. G., "Laminar Boundary Layer Stability Experiments on a Cone at Mach 8, Part 1: Sharp Cone," AIAA Paper 83-1761, July 1983.
[61] Jewell, J. S., and Kimmel, R. L., "Boundary Layer Stability Analysis for Stetson's Mach 6 Blunt Cone Experiments," AIAA Journal of Spacecraft and Rockets, vol. 54, no. 1, January-February 2017, pp. 258-265.
[62] Stetson, K. F., "Mach 6 Experiments of Transition on a Cone at Angle of Attack," *AIAA Journal of Spacecraft and Rockets*, vol. 19, no. 5, Sep.-Oct. 1982, pp. 397-403.
[63] Willems, S,. Gülhan, A., Juliano, T. J., and Schneider, S. P., "Laminar to turbulent transition on the HIFiRE-1 cone at Mach 7 and high angle of attack," AIAA 2014-0428, January 2014.
[64] Juliano, T. J., Kimmel, R. L., Willems, S. Gülhan, A., and Schneider, S. P., "HIFiRE-1 Surface Pressure Fluctuations from High Reynolds, High Angle Ground Test," AIAA paper 2014-0429, January 2014.
[65] Juliano, T. J., Kimmel, R. L., Willems, S., Gülhan, A., and Wagnild, R. M., "HIFiRE-1 Boundary-Layer Transition: Ground Test Results and Stability Analysis," AIAA-2015-1736, 2015.
[66] Stetson, K. F., and Rushton, G. H., "Shock Tunnel Investigation of Boundary-Layer Transition at M=5.5," *AIAA Journal*, vol. 5, no. 5, May 1967, pp. 899-906.
[67] Marineau, E. C., Moraru, C. G., Lewis, D. R., Norris, J. D., Lafferty, J. L., Wagnild, R. M., and Smith, J. A., "Mach 10 Boundary-Layer Transition Experiments on Sharp and Blunted Cones," AIAA paper 2014-3108, June 2014.
[68] Holden, M. S., "Experimental Studies of the Effects of Asymmetric Transition on the Aerothermal Characteristics of Hypersonic Blunted Slender Cones," AIAA paper 1985-0325, January 1985.
[69] Schneider, S. P., "Effects of High-Speed Tunnel Noise on Laminar-Turbulent Transition," *Journal of Spacecraft and Rockets*, vol. 38, no. 3, May-June 2001, pp. 323-333.
[70] Holden, M. S., Bower, D., and Chadwick, K., "Measurements of Boundary Layer Transition on Cones at Angle of Attack for Mach Numbers from 11 to 13," AIAA-95-2294, June 1995.
[71] DiCristina, V., "Three-Dimensional Boundary Layer Transition on a Sharp 8° Cone at Mach 10," *AIAA Journal*, vol. 8, no. 5, May 1970, pp. 852-856.
[72] Creel, T. R., Beckwith, I. E., and Chen, F. J., "Transition on Swept Leading Edges at Mach 3.5," *AIAA J. Aircraft*, vol. 24, no. 10, Oct. 1987, pp. 710-717.
[73] Gosse, R., and Kimmel, R., "CFD Study of Three-Dimensional Hypersonic Laminar Boundary Layer Transition on a Mach 8 Elliptic Cone," AIAA paper 2009-4053, June 2009.
[74] Neel, I. T., Leidy, A. N. and Bowersox, R. D. W., "Preliminary Study of the Effect of Environmental Disturbances on Hypersonic Crossflow Instability on the HIFiRE-5 Elliptic Cone," AIAA paper 20017-0767, January 2017.
[75] Li, F., Choudhari, M., Chang, C.-L., White, J., Kimmel, R., Adamczak, D., Borg, M., Stanfield, S., and Smith, M., "Stability Analysis for HIFiRE Experiments," AIAA paper 2012-2961, June 2012.
[76] Moyes, A. J., Kocian, T. S., Mullen, and Reed, H. L., "Boundary Layer Stability Analysis of HIFiRE-5b Flight Geometry," AIAA paper 2017-4301, June 2017.